

Liquid crystal lens with large focal length tunability and low operating voltage

Hongwen Ren, David W. Fox, Benjamin Wu, and Shin-Tson Wu

College of Optics and Photonics, University of Central Florida, Orlando, Florida 32816
swu@mail.ucf.edu

Abstract: We demonstrate a tunable focus liquid crystal (LC) lens by sandwiching a homogeneous LC layer between a planar electrode and a curved electrode. The curved electrode which is made of conductive polymer has parabolic shape with a large apex distance. Such design dramatically reduces the phase loss which leads to a short focal length (~15 cm). By using a thin top glass substrate on the curved electrode side, the operating voltage of the lens cell for achieving the shortest focal length is reduced to $\sim 23 V_{\text{rms}}$. This LC lens has advantages in large focal length tunability, low operating voltage, and good mechanical stability.

©2007 Optical Society of America

OCIS codes: (010.1080) adaptive optics; (160.3710) Liquid crystals; (220.3620) lens design

References and links

1. S. Sato, "Liquid-crystal lens-cells with variable focal length," *Jpn. J. Appl. Phys.* **18**, 1679-1684 (1979).
2. H. Ren, D. W. Fox, P. A. Anderson, B. Wu, and S. T. Wu, "Tunable-focus liquid lens controlled using a servo motor," *Opt. Express* **14**, 8031-8036 (2006).
3. H. Ren and S. T. Wu, "Variable-focus liquid lens," *Opt. Express* **15**, 5931-5936 (2007).
4. W. L. IJzerman, S. T. de Zwart, and T. Dekker, "Design of 2D/3D switchable displays," *SID Symposium Digest*, **36**, 98-101 (2005).
5. S. Suyama, M. Date, and H. Takada, "Three-dimensional display system with dual-frequency liquid-crystal varifocal lens," *Jpn. J. Appl. Phys. Part 1*, **38**, 480-484 (2000).
6. M. Hain, R. Glockner, S. Bhattacharya, D. Dias, S. Stankovic, and T. Tschudi "Fast switching liquid crystal lenses for a dual focus digital versatile disc pickup," *Opt. Commun.* **188**, 291-299 (2001).
7. T. L. Kelly, A. F. Naumov, M. Yu. Loktev, and M. A. Rakhmatulin, "Focusing of astigmatic laser diode beam by combination of adaptive liquid crystal lenses," *Opt. Commun.* **181**, 295-301 (2000).
8. H. Ren and S. T. Wu, "Inhomogeneous polymer-dispersed liquid crystals with gradient refractive index," *Appl. Phys. Lett.* **81**, 3537-3539 (2002).
9. H. Ren, Y. H. Fan, and S. T. Wu, "Tunable Fresnel lens using nanoscale polymer-dispersed liquid crystals," *Appl. Phys. Lett.* **83**, 1515-1517 (2003).
10. B. Wang, M. Ye, M. Honma, T. Nose, and S. Sato, "Liquid crystal lens with spherical electrode," *Jpn. J. Appl. Phys.* **41**, L1232-L1233 (2002).
11. H. Ren, Y. H. Fan, S. Gauza, and S. T. Wu, "Tunable flat liquid crystal spherical lens," *Appl. Phys. Lett.* **84**, 4789-4791 (2004).
12. B. Wang, M. Ye, and S. Sato, "Lens of electrically controllable focal length made by a glass lens and liquid crystal layers," *Appl. Opt.* **43**, 3420-3425 (2004).
13. B. Wang, M. Ye, and S. Sato, "Experimental and numerical studies on liquid crystal lens with spherical electrode," *Mol. Cryst. Liq. Cryst.*, **433**, 217-227 (2005).
14. Y. H. Fan, H. Ren, X. Liang, H. Wang, and S. T. Wu, "Liquid crystal microlens arrays with switchable positive and negative focal lengths," *J. Display Technology*, **1**, 151-156 (2005).
15. H. Ren and S. T. Wu, "Adaptive liquid crystal lens with large focal length tunability," *Opt. Express* **14**, 11292-11298 (2006).
16. I. Bruce, "Concerning drops," *Am. J. Phys.* **52**, 1102-1105 (1984).
17. S. Vafaei and M. Z. Podowski, "Theoretical analysis on the effect of liquid droplet geometry on contact angle," *Nuclear Engineering and Design* **235**, 1293-1301 (2005).
18. S. T. Wu, U. Efron, and L. D. Hess, "Birefringence measurements of liquid crystals," *Appl. Opt.* **23**, 3911-3915 (1984).
19. S. Gauza, H. Wang, C. H. Wen, S. T. Wu, A. J. Seed and R. Dąbrowski, "High birefringence isothiocyanato tolane liquid crystals," *Jpn. J. Appl. Phys. Part 1*, **42**, 3463-3466 (2003).
20. A. Spadło, R. Dąbrowski, M. Filipowicz, Z. Stolarz, J. Przedmojski, S. Gauza, Y. H. Fan, and S. T. Wu "Synthesis, mesomorphic and optical properties of isothiocyanatotolanes," *Liq. Cryst.* **30**, 191-198 (2003).

1 . Introduction

Adaptive-focus lens has found useful applications in image processing [1-3], displays [4,5], and optoelectronic devices [6, 7]. Unlike a mechanical zoom lens, the focal length of a liquid crystal (LC) lens can be tuned electrically [8-9]. A simple method to make an LC lens is to use a curved and a flat indium-tin-oxide (ITO) electrode [10-15] to generate a gradient refractive index profile on a homogeneous LC layer. Because of the uniform cell gap the lens is free from light scattering and has uniform response time. Usually the curved electrode has a spherical shape, thus, the applied voltage across the electrodes generates a centro-symmetric inhomogeneous electric field within the LC layer. Such an LC layer exhibits focusing property due to the generated gradient refractive index profile. The focal length of the LC lens depends on the phase gradient. Our theoretical analysis [15] indicates that if the gap between the spherical ITO electrode and the LC cell is filled with glass or polymer, then the generated electric field gradient within the LC layer is relatively shallow which leads to a long focal length. To shorten the focal length, we proposed to use a glass shell instead of a glass lens [15]. If the sag of the glass shell is filled with air, the generated electric field gradient within the LC layer is greatly enhanced as compared to the glass shell filled with polymer. However, the glass shell is fragile and its mechanical stability is a concern. Furthermore, the glass shell brings two additional surfaces so that the reflection loss is increased.

In this paper, we demonstrate a tunable-focus LC lens using a parabolic electrode. Our parabolic electrode, made of conductive polymer, has a large ratio between the apex distance and the base radius. This sharp phase gradient dramatically reduces the phase loss. As a result, the shortest focal length achievable is ~ 15 cm. By using a thin (0.21 mm) glass substrate on the curved electrode side, the operating voltage of the LC lens is reduced from 140 V_{rms} [15] to ~ 23 V_{rms}. This is an important step toward practical applications for cell phone zoom lens.

2. Fabrication of parabolic electrode

To fabricate a parabolic electrode, we first prepared a parabolic polymer structure. It is known that when a droplet of liquid falls on the surface of a horizontally placed substrate, the droplet presents a “parabolic” shape [16,17] as depicted in Fig. 1(a). Depending on the surface tension of the substrate and the liquid, the exact surface profile may deviate slightly from a perfect parabola. However, the apex distance (AD) shown in Fig. 1(a) is usually short.

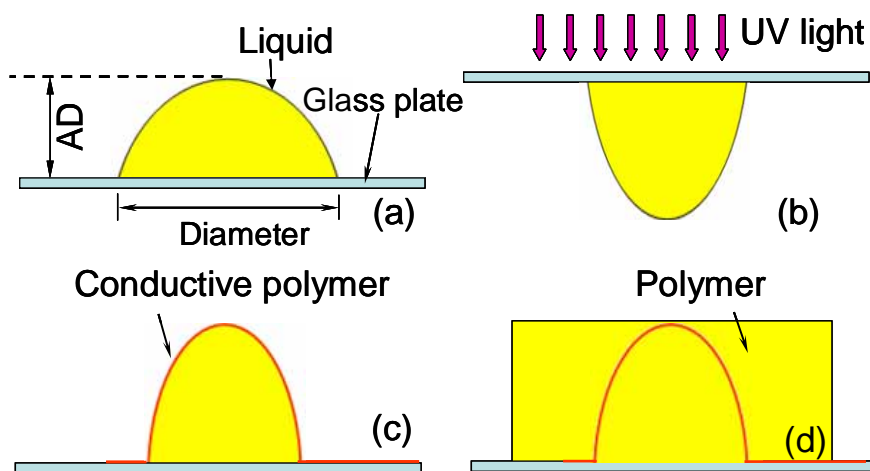


Fig. 1. Fabrication process of parabolic electrode: (a) put a drop of prepolymer on the top substrate surface, (b) turn the substrate up-side down and cure the polymer by UV light, (c) coat a conductive polymer layer as electrode, and (d) flatten the lens surface by the same polymer.

To increase AD, we turned the substrate up-side down as shown in Fig. 1(b) and let gravity force elongate the droplet shape in the vertical direction. The droplet material we used is NOA81 (Norland Optical Adhesive) which is a photosensitive prepolymer, and we polymerized the droplet using a UV light, as Fig. 1(b) shows. After complete polymerization, the lens-like droplet is solidified. The polymeric lens formed under these conditions has a smooth surface.

Next we coated a water-based conductive polymer on the solid lens surface, as shown in Fig. 1(c). The conductive polymer has good optical performance as an ITO electrode. Moreover, its refractive index is similar to that of the polymeric lens material.

Due to the non-spherical shape, such a lens usually has large distortion. To avoid this problem, we filled the substrate surface using the same polymeric material, as Fig. 1(d) shows, so that the substrate became flat. After photo-polymerization, the polymer electrode was embedded inside the polymer substrate except for the lead contact.

To prepare a LC lens, we used this substrate as the top electrode and an ITO glass as the bottom substrate. The inner surfaces of the cell were coated with a thin polyimide layer and buffed in anti-parallel directions. When the cell is filled with a nematic LC, the LC cell presents a homogeneous alignment along substrate surface, as shown in Fig. 2. Because the refractive index of NOA 81 ($n_p=1.52$) matches well with that of the glass substrate ($n_g=1.52$), the Fresnel reflection between interfaces is minimized.

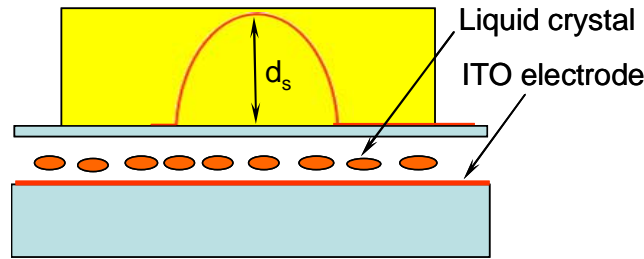


Fig. 2. Device structure of a LC lens cell. The top electrode is a conducting polymer and bottom electrode is ITO.

3. Lens design principles

When a voltage (V) is applied to the electrodes, the LC layer experiences an inhomogeneous electric field because the top electrode has a curved shape. According to our previous analysis, within the LC layer the electric field at the border (E_b) and center (E_c) can be expressed as [15]:

$$E_b = \frac{V}{\epsilon_{LC}} / \left(\frac{d_{LC}}{\epsilon_{LC}} + \frac{d_g}{\epsilon_g} \right), \quad (1)$$

$$E_c = \frac{V}{\epsilon_{LC}} / \left(\frac{d_{LC}}{\epsilon_{LC}} + \frac{d_g}{\epsilon_g} + \frac{d_s}{\epsilon_p} \right). \quad (2)$$

In Eqs. (1) and (2), d_{LC} , d_g , and d_s represent the LC layer thickness, the top glass substrate thickness, and the apex distance of the curved electrode, and ϵ_{LC} , ϵ_g , and ϵ_p represent the dielectric constant of the LC medium, the top glass plate, and the filled polymer, respectively.

From Eqs. (1) and (2), for a given applied voltage, the electric field in the center is always weaker than that near the edges because of the parabolic electrode. Therefore, to maximize the phase difference between the lens edges and center, ideally we should let the LC directors be fully reoriented at the borders but keep those in the center below or near threshold. In a LC lens cell, if the LC material and cell gap are chosen, i.e., d_{LC}/ϵ_{LC} is fixed, then increasing d_g or d_s would lower E_c . However, increasing d_g will cause the operating voltage to increase. In

order to obtain a short focal length while keeping a low operating voltage, a good approach is to decrease d_g and increase d_s at the same time.

4. Experiment and results

4.1 Polymer lenses

To test our hypotheses described in Figs. 1(a) and 1(b), we fabricated two polymer lenses for comparison. Firstly, a thin PDMS membrane film was coated on a glass substrate surface; then a small amount of NOA 81 was dropped on the PDMS surface. We chose PDMS rather than glass as the contacting surface for two reasons: it has a relatively large contact angle with NOA 81 and it is easy to peel off the lens without any damage. Before UV exposure, the weight of the first droplet was measured to be 31.0 mg and the second droplet was 31.3 mg. The first droplet was UV cured while it was placed in the upright position, as shown in Fig. 1(a). The second droplet was UV cured in the up-side down position, as shown in Fig. 1(b). After polymerization, the two lenses were solidified. The bottom radius and apex distance of the first and second lenses were measured to be (2.75 mm and 1.27 mm) and (2.1 mm and 2.7 mm), respectively. To probe the lens profiles, we used a collimated He-Ne laser beam to illuminate the lens, as shown in Fig. 3. A CCD camera was placed right behind the lens. The blocked light by the lens gives the side view profile of the lens.

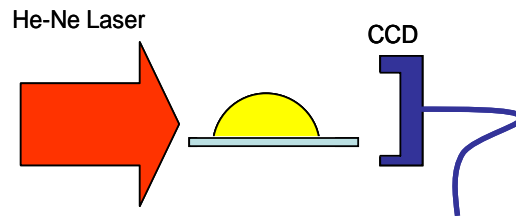


Fig. 3. Method for measuring the lens profile.

Figures 4(a) and 4(b) show the side view profiles of the two polymeric lenses, respectively. The shape of each lens is centro-symmetric, but the second one has a longer apex distance. Suppose we use the same volume to prepare a semi-spherical ball lens and its radius of the base area is 2.1 mm, then the apex distance of the semi-ball lens should be 2.1 mm. Our second lens has an apex distance of 2.7 mm, which is larger than the radius (2.1 mm) of its base. Therefore, the second lens indeed has a parabolic surface profile.

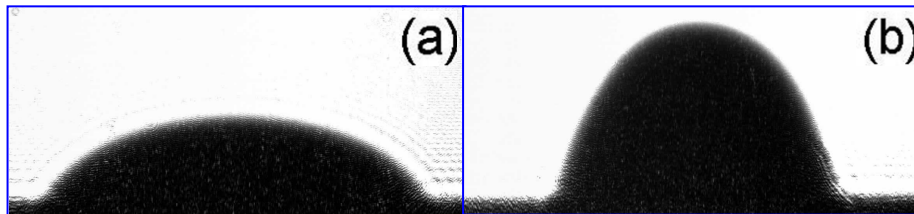


Fig. 4. Measured side-view profiles of two polymeric lenses fabricated according to Figs. 1(a) and 1(b).

4.2 The parameters of LC lens cell

According to Fig. 2, we prepared a lens cell with a homogeneous LC layer. The parameters of the LC cell are listed as follows: LC BL-003 ($\Delta\epsilon=17$, $\epsilon_{//}=22.1$, $\Delta n=0.261$; purchased from Merck and used as received), $d_{LC}\sim 60\ \mu\text{m}$, $d_g=0.21\ \text{mm}$. The radius of the base area is 2.1 mm and the apex distance of the conductive polymer is 2.7 mm. The total thickness of the lens cell is $\sim 3.75\ \text{mm}$. The material we chose for the curved electrode is water-based conductive polymer ELP-3040 (purchased from Agfa-Gevaert, Belgium). This conductive polymer has the following properties: (1) its conductivity is as good as an ITO electrode, (2) it is easy to form a thin film and tightly adhere to the polymer or glass substrate surface, (3) it has high

transmittance in the visible, and (4) its refractive index matches well with that of conventional polymer or glass material.

4.3 Lens performances

To evaluate the lens performance, we first observed the interference rings of the lens cell using a microscope. The sample was placed between two crossed polarizers. The rubbing direction of the lens cell was oriented at 45° with respect to the fast axis of the linear polarizer. Because the lens aperture is relatively large, only a portion of the lens is shown. At the null voltage state, the sample generates 3 interference rings, as shown in Fig. 5(a). This result indicates that the LC layer initially has a lens character but its focal length is very long (>1.3 m). When an external voltage above $3.5 V_{\text{rms}}$ was applied to the electrodes, interference rings begin to be generated from the lens border. Figure 5(b) shows the observed interference pattern at $5 V_{\text{rms}}$. Even at such a low voltage, more than 6 concentric circular rings are generated from the lens border. Increasing the applied voltage would produce more rings and those rings are spread from border to center. At $23 V_{\text{rms}}$, the number of rings reaches a maximum, as shown in Fig. 5(c). Keeping on increasing voltage will cause the ring in the center to swell. This result means at $V=23 V_{\text{rms}}$ the gradient of the refractive index distribution within LC layer is the largest. As the applied voltage increases, the interference rings begin to disappear in the center and the ring density becomes looser. At $V=35 V_{\text{rms}}$, the interference rings near the lens border become the loosest and will not move toward the center. These rings are shown in the up-left corner in Fig. 5(d). Such results imply that the orientation of LC directors near the lens border have reached a saturation level. In our lens cell the interference rings induced by the external voltage are highly symmetrical and circular, and the distribution of the rings from center to border is harmonious which means the spherical aberration generated by the LC layer itself is negligible.

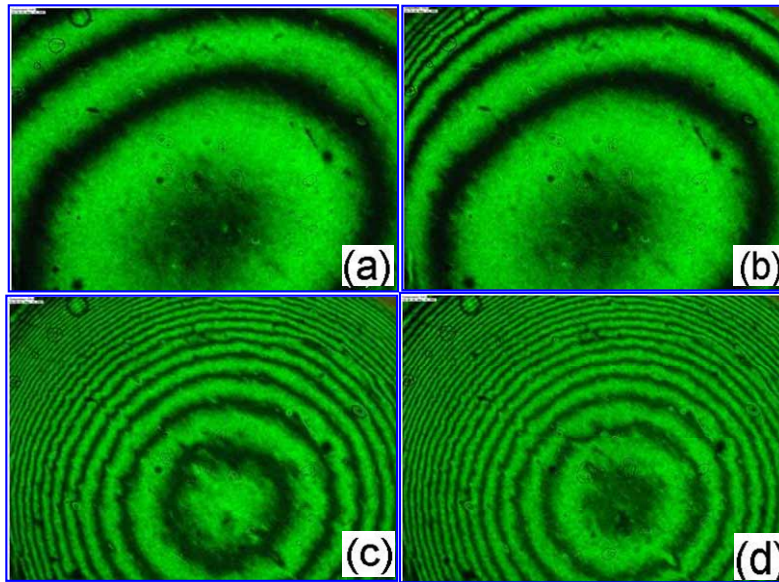


Fig. 5. Observed microscope interference fringes of the LC lens at (a) $V=0$, (b) $V=5$, (c) $V=23$, and (d) $35 V_{\text{rms}}$.

From the interference rings shown in Fig. 5, we can calculate the phase profile across the lens aperture. Figure 6 shows the relative phase retardation profiles at $V=5$ and $23 V_{\text{rms}}$. The curve at $V=5 V_{\text{rms}}$ (red) is almost flat near the center because the LC molecules near the lens center still keep homogeneous alignment. Under such a condition, the spherical aberration is large. On the other hand, at $V=23 V_{\text{rms}}$ the curve presents a bell shape. Due to the large gradient electric field within the LC layer, the induced bell-shaped phase profile is sharp. In

this case, almost all the LC molecules from the lens border to the lens center contribute to the light focusing behavior. Thus, its focal length is short.

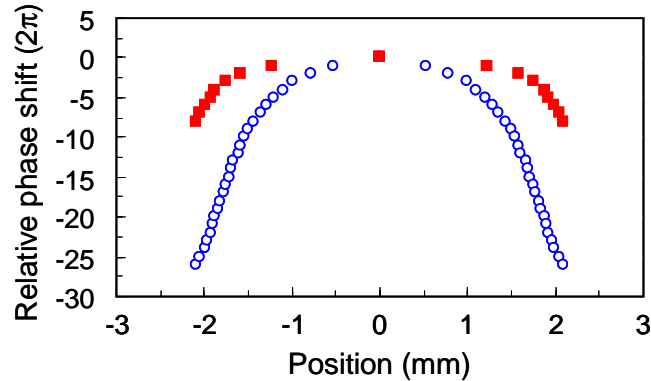


Fig. 6. Relative phase retardation profiles at $V=5 V_{rms}$ (red) and $V=23 V_{rms}$ (blue).

To estimate the phase loss of the LC lens, we calculated the phase retardation according to the following formula [18]:

$$\delta = 2\pi d_{LC} \Delta n / \lambda \quad (3)$$

where λ is the wavelength. From the aforementioned lens parameters, ($d_{LC} \sim 60 \mu\text{m}$, $\Delta n \sim 0.261$, and $\lambda = 0.55 \mu\text{m}$), we find the maximum phase difference is $\Delta\delta \sim 28 \times 2\pi$, i.e., 28 rings. From the experimental result shown in Fig. 6, our lens cell generates 26 rings, which is very close to the theoretical value. In the previous LC lenses employing a spherical electrode, the obtained available phase change is lower than 42% of its theoretical value [11-14] because the electric field gradient is too shallow. In our design, the achievable LC phase reaches $\sim 93\%$ due to the large gradient electric field generated in the LC bulk. Because of this improved efficiency, a thinner cell gap ($\sim 60 \mu\text{m}$ as compared to $\sim 300 \mu\text{m}$) can be used in our design which, in turn, significantly reduces the switching time of the lens.

To observe the image property of the lens cell, we typed “1432” on a card as an object and the lens was set at ~ 7 cm in front of the object. Since the LC lens works for a linearly polarized light, a linear polarizer sheet was placed between the sample and the object. The rubbing direction of the LC cell was adjusted to be parallel to the optic axis of the polarizer. A digital camera was placed right behind the sample. Two images were taken at $V=0$ and $V=25 V_{rms}$, as shown in Figs. 7(a) and 7(b), respectively. Through the lens aperture, at $V=0$ the letter “432” is located near the center. At $V=25 V_{rms}$, the image is magnified. Because the distance of the object to the LC lens is shorter than the focal length of the LC lens, the observed image is upright but virtual. In this experiment, the f-number of the LC lens is estimated to be $\sim f/40$. Since the lens aperture ($D=4.2$ mm) is relatively large, the magnification ratio is not very large. Decreasing the lens aperture will significantly enhance the lens focusing power.

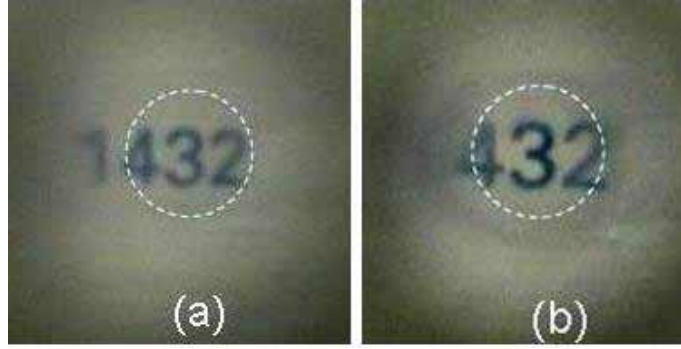


Fig. 7. Imaging behavior of the LC lens at (a) $V=0$ and (b) $V=25 V_{rms}$.

In our lens cell, the top polymer substrate (the yellow part in Fig. 2) is only ~ 3 mm so that its contribution to the spherical aberration is insignificant. If the lens aperture is reduced, then the polymer substrate thickness could be reduced proportionally. As a result, its contribution to the LC lens aberration would be smaller.

The focal length of the lens cell was calculated based on the measured interference fringes at different voltages, as shown below:

$$f = r^2 / 2\lambda N \quad (4)$$

where r is the radius of the lens aperture and $N (=d_{LC}\Delta n/\lambda)$ is the number of the observed rings. From ring counting and Eq. (4), the relationship between the focal length of the LC lens and the applied voltage is plotted in Fig. 8. At null voltage, the inherent focal length of the LC lens is very long. As the voltage increases, the focal length is shortened dramatically. At $V \sim 23 V_{rms}$, the focal length reaches the shortest (~ 15.4 cm). Further increasing the voltage would cause the focal length to bounce back, but at a much slower rate.

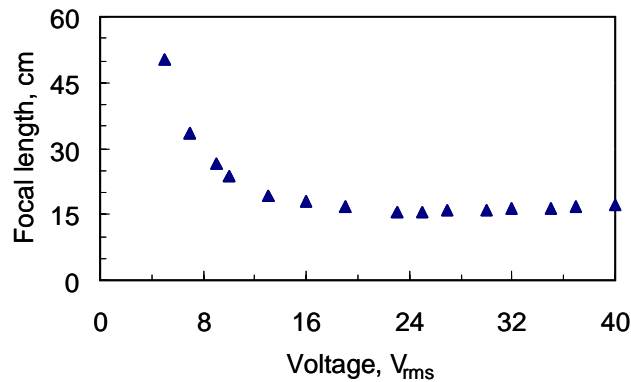


Fig. 8. Voltage dependent focal length of the LC lens.

The switching time of the lens depends on the LC cell gap. In our experiments, the thickness of the LC layer is $d_{LC} \sim 60 \mu\text{m}$ and the estimated response time is $\sim 4\text{s}$. To improve the response time, we could use a high birefringence LC [19,20] for reducing the cell gap. From Eq. (1), and Eq. (2), the external voltage for achieving the shortest focal length can be further decreased if we replace the present 0.21 mm top glass substrate by a thinner substrate. However, these thin substrates are more fragile.

5. Conclusion

We have demonstrated an electrically tunable focus lens by sandwiching a homogeneous LC layer between a planar electrode and a parabolic electrode. Our design shows a very small

phase loss. The shortest focal length achieved is ~15 cm. By choosing a thin glass plate as the top glass substrate of the lens cell, we can further reduce the operating voltage. Our LC lens possesses the following attractive features: a wide focal length tunability, low operating voltage, good mechanical stability, and easy fabrication. A potential application of this kind of lens for cell phone cameras is foreseeable.